



Article

Improved Boreal Forest Wildfire Fuel Type Mapping in Interior Alaska Using AVIRIS-NG Hyperspectral Data

Christopher William Smith ^{1,*}, Santosh K. Panda ¹ , Uma Suren Bhatt ¹ and Franz J. Meyer ^{1,2}

¹ Geophysical Institute, University of Alaska Fairbanks, Fairbanks, AK 99775, USA; skpanda@alaska.edu (S.K.P.); usbhatt@alaska.edu (U.S.B.); fjmeyer@alaska.edu (F.J.M.)

² Alaska Satellite Facility, University of Alaska Fairbanks, Fairbanks, AK 99775, USA

* Correspondence: cwsmith9@alaska.edu

Abstract: In Alaska the current wildfire fuel map products were generated from low spatial (30 m) and spectral resolution (11 bands) Landsat 8 satellite imagery which resulted in map products that not only lack the granularity but also have insufficient accuracy to be effective in fire and fuel management at a local scale. In this study we used higher spatial and spectral resolution AVIRIS-NG hyperspectral data (acquired as part of the NASA ABoVE project campaign) to generate boreal forest vegetation and fire fuel maps. Based on our field plot data, random forest classified images derived from 304 AVIRIS-NG bands at Viereck IV level (Alaska Vegetation Classification) had an 80% accuracy compared to the 33% accuracy of the LANDFIRE's Existing Vegetation Type (EVT) product derived from Landsat 8. Not only did our product more accurately classify fire fuels but was also able to identify 20 dominant vegetation classes (percent cover >1%) while the EVT product only identified 8 dominant classes within the study area. This study demonstrated that highly detailed and accurate fire fuel maps can be created at local sites where AVIRIS-NG is available and can provide valuable decision-support information to fire managers to combat wildfires.



Citation: Smith, C.W.; Panda, S.K.; Bhatt, U.S.; Meyer, F.J. Improved Boreal Forest Wildfire Fuel Type Mapping in Interior Alaska Using AVIRIS-NG Hyperspectral Data. *Remote Sens.* **2021**, *13*, 897. <https://doi.org/10.3390/rs13050897>

Academic Editor: Luke Wallace

Received: 31 December 2020

Accepted: 24 February 2021

Published: 27 February 2021

Publisher's Note: MDPI stays neutral with regard to jurisdictional claims in published maps and institutional affiliations.



Copyright: © 2021 by the authors. Licensee MDPI, Basel, Switzerland. This article is an open access article distributed under the terms and conditions of the Creative Commons Attribution (CC BY) license (<https://creativecommons.org/licenses/by/4.0/>).

Keywords: AVIRIS-NG; hyperspectral; random forest; fire fuel; boreal forest; remote sensing

1. Introduction

The boreal forest makes up 11% of the Earth's land surface spanning over three continents making it the largest terrestrial ecosystem in the world [1]. Boreal forest covers half of Alaska and fire is a natural feature of the boreal ecosystem. More acres are burning as Alaska's fire environment is changing in response to hot and dry summers, longer growing seasons and shifts in seasonal precipitation [2]. In the boreal forest, the ability to accurately map spruce, hardwoods, mixedwood forests and tundra is critical for understanding the potential and growth of a wildfire [3]. Currently in Alaska, the land and resource management agencies (Bureau of Land Management, National Park Service, Bureau of Indian Affairs, US Forest Service) and wildfire suppression agencies (Alaska Fire Services, Alaska Division of Forestry, and US Forest Service) use the 2014 LANDFIRE (LF) geospatial products for land and resource management as well as for fuel and wildfire management LF (a U.S. government interagency program) provides geospatial layers for land resource planning, management, and operations including management of active wildfires, wildfire fuels, and firefighter safety. However, the LF geospatial products for Alaska, particularly vegetation and fuel maps, lack the granularity and accuracy to be effective in wildfire and fuel management at local scale as these products are derived from coarser spatial and spectral resolution Landsat 8 satellite images [4].

Wildfires in Alaska pose a serious threat to critical infrastructure, private property, subsistence resources, and human health and life [2]. In 2019 alone Alaska experienced 378 lightning-caused fires that burned 2,525,356 acres [5]. With the onset of global climate change, the circumpolar north has experienced a temperature change 1.5 to 4.5 times higher than the global average in the last half-century [2,6]. The intensification of global

climate change further increases the likelihood of boreal forest fires due to the warming summer temperatures (hot, dry and windy condition), the onset of earlier snowmelt that lengthens the fire season, and precipitation variability. Consequently, leading to an increase in the frequency, severity, and duration of wildfires [7–10]. In the last two decades (2001–2020) wildfires in Alaska burned 31.4 million acres (i.e., 2.5 times more acres burned than during the previous two decades—1981–2000: 14.1 million acres burned). Fires also release greenhouse gases such as CO₂ that contribute to a positive feedback loop affecting climate-driven changes that affect boreal forest fires [11]. Between 1985–2015 Alaska has experienced increasing temperature and lightning activity across the state [12]. This increase in lightning activity is concerning considering that lightning-caused ignitions and acres burned have been increasing since 1975 [13]. This rapidly changing fire environment necessitates the need for more frequent monitoring efforts using remote sensing data products that assess ecosystem changes such as changes in vegetation, fuel types, and fire risk [2].

Hyperspectral data is one promising remote sensing resource that has been used for mapping vegetation and its attributes with high accuracy in many different parts of the world [14–20]. In the Florida Everglades, by combining hyperspectral with lidar data Zhang et al. were able to map wetland vegetation with an 86% accuracy [20]. NASA's latest Airborne Visible/Infrared Imaging Spectrometer Next-Generation (AVIRIS-NG) hyperspectral camera has 425 spectral bands within the wavelength range 400–2500 nm, and higher pixel resolution 5–10 m depending on the flying height [21]. AVIRIS-NG camera has been flown in many parts of the world to study natural vegetation, crop health, and ecosystem processes [14,16,18,19,22]. In an agricultural setting AVIRIS-NG has been used to quantify plant chlorophyll and identify spectral differences in crop types [19], and for mapping crops species [18]. AVIRIS-NG has also been employed in natural settings to generate products that evaluate forest ecosystems such as by mapping stress of mangrove forests [16] and forest vegetation across a landscape [14]. All of the aforementioned studies show the potential of AVIRIS-NG for mapping vegetation type and vegetation health with higher accuracy to support effective land and resource management for a variety of applications including wildfires. In 2018, the AVIRIS-NG camera was flown for the first time over Alaskan boreal forest as part of NASA's Arctic-Boreal Vulnerability Experiment (ABOVE) project campaign. In Alaska AVIRIS-NG has been used to map vegetation recovery following a fire [22]. However, we are not aware of any study using AVIRIS-NG data for fuel mapping in Alaskan boreal forest.

Currently in Alaska, the best geospatial products that are available to fire managers are the LANDFIRE program's vegetation and fire fuel maps. A major problem with the LF Program's 2014 map products is that it was created using Landsat 30 m multi-spectral imagery and not adequately field validated [23,24]. Due to the low spatial and spectral resolutions of the Landsat imagery, the LF map products lack detail and granularity that is required for reliable wildfire risk assessment and management at local scale (Figure 1). The AVIRIS-NG hyperspectral data collected as part of the NASA's ABOVE project campaign has high spectral (425 bands) and spatial (5 m) resolutions; it offers detailed spectral signatures for vegetation that helps discriminate vegetation types based on spectral signatures alone (Figure 1). The image classifiers exploit the detailed spectral signatures and the fine differences in signatures between vegetation types to identify a pixel's vegetation class accurately. We hypothesize that the higher spatial and spectral resolution of hyperspectral data would allow for highly accurate and detailed maps of fire fuel. So, the goal of this research was to use AVIRIS-NG hyperspectral imagery to create detailed and improved vegetation and fuel type maps that are better suited for effective wildfire risk assessment and management (at local scale) than the existing products from LF.

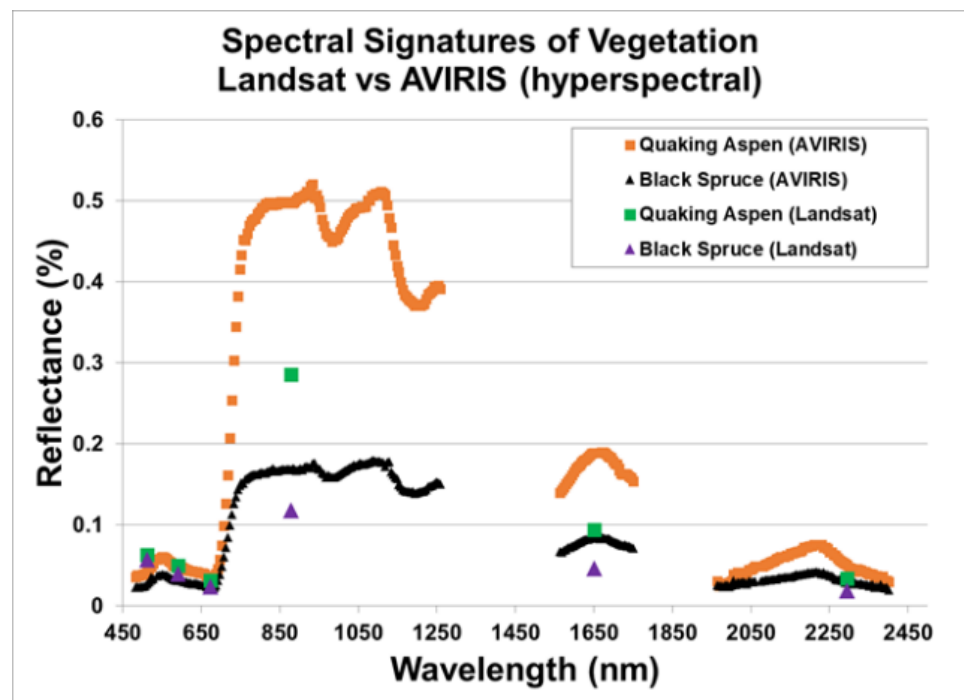


Figure 1. Comparison of spectral signatures of two distinct vegetation classes extracted from hyperspectral AVIRIS-NG and multispectral Landsat 8 data. The AVIRIS-NG spectral signature is more unique between different vegetation classes.

2. Materials and Methods

2.1. Study Area

Bonanza Creek Experimental Forest (BCEF) and Caribou-Poker Creeks Research Watershed (CPCRW), were identified as the study sites because of their accessibility and high vegetation/fuel diversity. BCEF, a site established in 1963, is located 20 km southwest of Fairbanks and CPCRW is located 50 km north of Fairbanks; both sites are located in the discontinuous permafrost zone (Figure 2). Also, both BCEF and CPCRW sites have a history of scientific research focused on boreal forest ecosystem structure and function, including ecosystem succession following forest fires. BCEF contains 4 distinct topographic zones (upland hills and ridges, lowland toe slopes and valley bottoms, old Tanana River terraces, and the active floodplain) and contains a wide range of forested and non-forested vegetation. In CPCRW south facing slopes and uplands are dominated by hardwood forest (*Betula papyrifera*, *Populus tremuloides*), north facing slopes have black spruce (*Picea mariana*) and alder (*Alnus viridis*). Dwarf shrubs (*Betula nana*, *Salix* sp., *Vaccinium uliginosum*) and alder (*Alnus tenuifolia*) dominate the lowlands [25]. Therefore, these sites are ideal for testing different datasets and methods for detailed mapping of boreal vegetation and other attributes that can be used to assess fire fuel status because they include a majority of the dominant vegetation classes found in the Alaskan boreal forest ecosystem.



Figure 2. Map of the two study sites in relationship to the Alaskan Boreal Forest and Fairbanks. CPRW is located 50 km North of Fairbanks and BCEF is located 20 km Southwest of Fairbanks.

2.2. Data

AVIRIS-NG hyperspectral data collected in July 2018 as part of the NASA ABoVE project is available for both study sites [21]. Both BCEF and CPRW images were collected on 23 July 2018. Also, we used the 2 m Arctic Digital Elevation Model (DEM) from the Polar Geospatial Center (University of Minnesota, Saint Paul, MN, USA). At BCEF we additionally used a Landsat 8 surface reflectance scene (Path: 70 Row: 15 Scene ID: LC80700152018206LGN00) collected on 25 July 2018 (source: <https://earthexplorer.usgs.gov/>). In the summer of 2019 and 2020, we surveyed vegetation at 42 plots (plot size: 10 m × 10 m) in BCEF and 36 plots in CPRW which were collected to be used as training data (Figure 3). At each location, we recorded the vegetation composition, the vegetation percent cover, canopy cover, understory cover, aspect, slope, and elevation. These plots were then classified into a Viereck level IV (Alaska Vegetation Class) and Alaska Fuel Model Guide Task Group (2018) fuel type. In the summer of 2020 we surveyed 55 locations in BCEF and 62 locations in CPRW that were randomly selected hiking in the woods and used for accuracy assessment (Figures 4 and 5). We recorded the dominant vegetation type and canopy cover at these random locations. We used a survey grade Trimble R10 RTK unit for geolocating all field locations. We used the 2019 field data to train the image classifiers and the 2020 field data for classification accuracy assessment. The two study sites (BCEF and CPRW) are part of protected state forests. The vegetation change in these sites due to natural succession takes places at a multi-decadal to century time scale. However, dramatic vegetation change can occur due to wildfires or insect outbreaks. During the field survey we did not observe any evidence of fire or insect outbreak within the study area. Also, we are not aware of any report of forest damage or change in the study areas since 2018 (when AVIRIS-NG image was collected). So we are confident that the use field data collected in 2019 for image classifier training and field data collected in 2020 for classification accuracy assessment are robust and resulted in accurate and reliable map products.

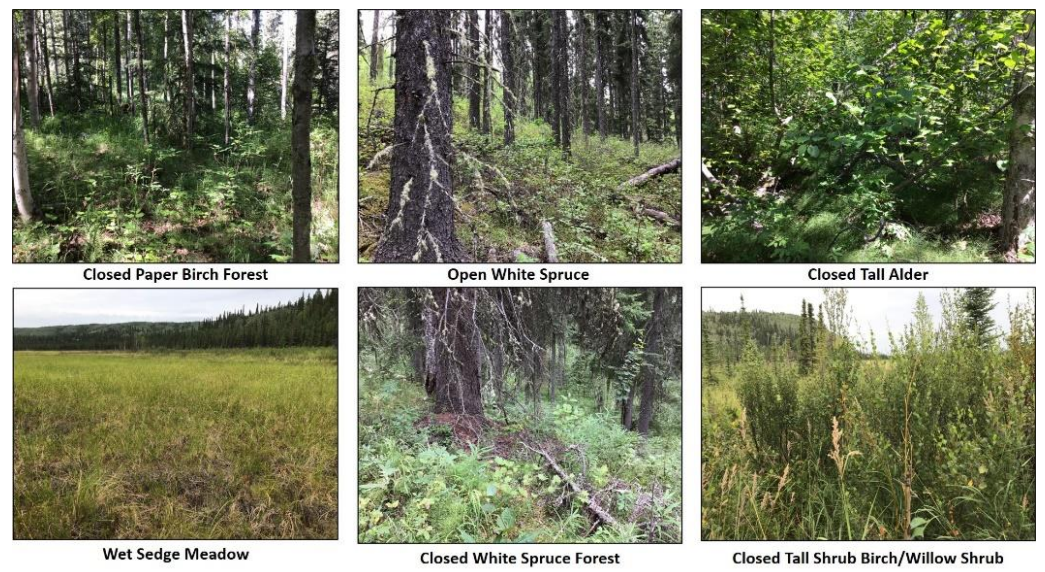


Figure 3. Field photos of select vegetation/fire fuel classes from interior Alaska.

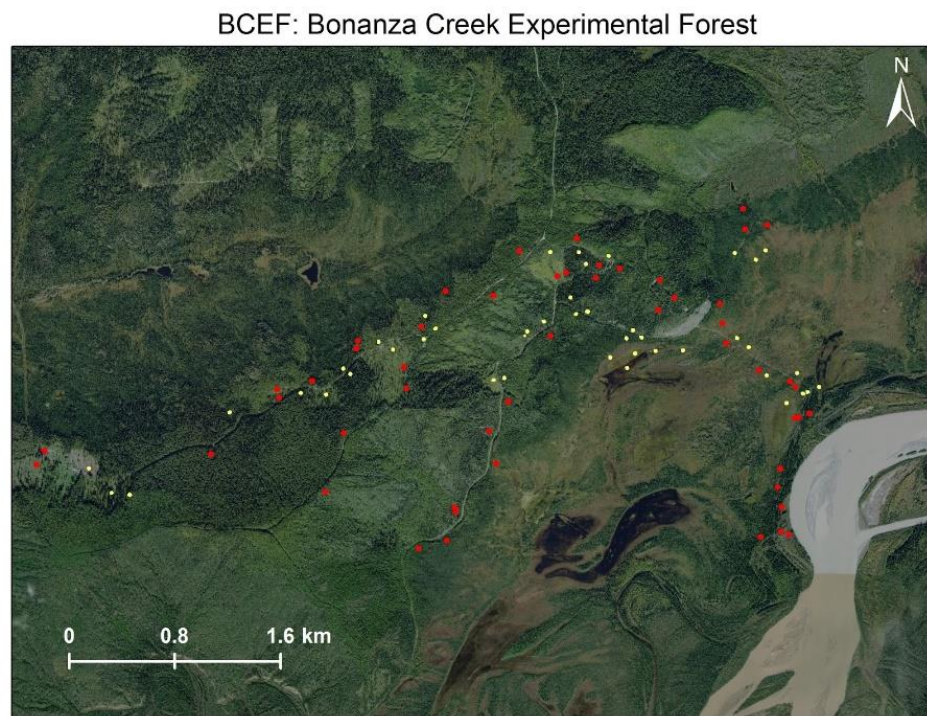


Figure 4. Map showing the 42 surveyed field plots (yellow) and 55 field locations (red) at BCEF.

CPCRW: Caribou-Poker Creeks Research Watershed



Figure 5. Map showing the 36 surveyed field plots (yellow) and 62 field locations (red) at CPCRW.

2.3. Preprocessing

The AVIRIS-NG sensor collects images in the wavelengths ranging from 380–2500 nm at 5 nm intervals (425 bands) and ~5 m spatial resolution. Some of these bands fall outside of the atmospheric windows and overlap with atmospheric absorption and scattering wavelengths. We removed these undesired bands (1260–1560 nm; 1760–1960 nm;) in order to minimize their influence on image classification [26]. Bands below 480 nm were found to be not useful in differentiating vegetation classes so they were also removed before further processing. Both study areas contain a number of non-vegetated land covers such as gravel roads, turbid river water, and lakes. Since our research was exclusively focused on vegetation classes, we removed non-vegetation land cover classes altogether in order to optimize data processing and analysis. We achieved this by masking out non-vegetated pixels using the Normalized Difference Vegetation Index (NDVI) calculated using the Equation $\frac{(\text{band } 97 - \text{band } 54)}{(\text{band } 97 + \text{band } 54)}$ with a threshold of NDVI < 0.5 (visual assessment) (Figure 6). We used ENVI 5.3 [27], QGIS 10.3 EnMAP-Box plugin [28], and ArcMap 10.7 [29] software for image processing and analyses.

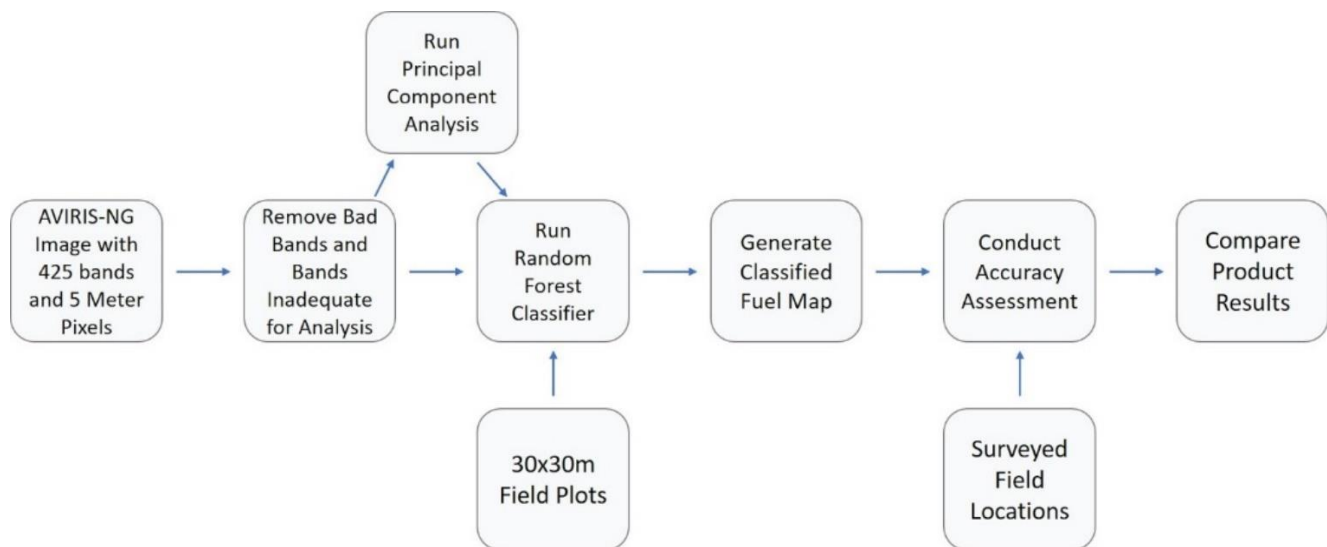


Figure 6. Workflow for AVIRIS-NG image preprocessing and vegetation classification.

2.4. Fire Fuel Mapping

Principal component analysis (PCA) is a technique used to reduce the data volume of a data set by removing redundant data while maintaining the variance of the data set and is often used on remotely sensed data [30]. In order to assess the significance of all bands and reduced PC bands in boreal vegetation mapping we ran PCA on AVIRIS-NG scenes from both study sites. We used the first five PC bands, which retained 99% of the total data variance. We classified vegetation to Viereck level IV and to a fire fuel type [31,32] using the 304 bands, the PCA bands+DEM, and a Landsat 8 image separately. We used the random forest classifier (trees: 500, 30 rules per tree) which is a supervised classification algorithm based on decision trees [33–37]. We selected the Random Forest classifier over other image classifiers as it performs better when a large amount of training data is available, less prone to overfitting, ideal for processing large volume of data, and results in higher accuracy products [34–37]. Several studies have demonstrated the success and effectiveness of the random forest classifier in vegetation mapping [33,37]. The 10 m × 10 m field plots surveyed in 2019 were used for training the classifier and the random points surveyed in 2020 for accuracy assessment. We calculated the area offset of the AVIRIS-NG scenes using five ground control points collected at CPCRW. The average offset was 5.5 ± 3.3 m and in order to account for this positional error we used the random points with a 5-m buffer to carry out the accuracy assessment on classified map products. We used QGIS 10.3 EnMAP-Box plugin [28] for RF classification on the 304-bands while the rest of the processing and analysis were done in ArcMap 10.7 [29].

3. Results

3.1. BCEF

Using the random forest classifier, we were able to map 25 different vegetation types and 17 fire fuel types from the BCEF AVIRIS-NG data (Table 1). We compared our vegetation map with the LF EVT map over the BCEF study site. Our vegetation map has 20 dominant vegetation classes (i.e., a class with 1% or more coverage) compared to eight vegetation classes in the LF EVT map (Figure 7 and Table 2). Based on Cohen's Kappa value all of our products had a moderate agreement (Kappa >0.40) and the AVIRIS-NG 304 bands had a strong agreement (Kappa \geq 0.70). We assessed the classification accuracy of our map products and the LF EVT map using field survey data. Of all source image data, the vegetation type (overall accuracy: 80%) and fuel type maps (overall accuracy: 81.5%) generated from the AVIRIS-NG 304 bands had the highest accuracy, followed by map products generated from Landsat+DEM and AVIRIS-NG PCA data (Table 3). The LF

EVT product had an overall accuracy of 33% (i.e., 14 plots out of 44 plots correctly mapped). In summary, our map products derived from the AVIRIS-NG 304 bands not only have an accuracy 2.5 times better than the existing LF EVT product, but also map vegetation and fuel types at a much higher detail.

Table 1. A list of vegetation types (fuel types) and their area percent cover mapped from AVIRIS-NG 304 band image at BCEF.

Vegetation Type	Fuel Type	Cover (%)
Black Spruce Woodland with Tussocks	Black Spruce Woodland w/Tussocks	3.71
Black Spruce/Tamarack Forest	Black Spruce-Tamarack Forest	3.08
Bluejoint	Bluejoint	0.12
Post Harvest Bluejoint	Bluejoint	0.71
Bluejoint/Shrub & Bluejoint Herb	Bluejoint-Shrub/Herb	2.95
Closed Black Spruce	Closed Black Spruce Forest and Closed Mixed Black Spruce-White Spruce Forest	10.33
Closed Black/White Spruce Forest	Closed Black Spruce Forest and Closed Mixed Black Spruce-White Spruce Forest	1.44
Closed Tall Alder	Closed Tall Alder-Willow	10.48
Closed Tall Shrub Birch/Willow Shrub	Closed Tall Birch Shrub	1.69
Closed White Spruce	Closed White Spruce Forest	3.28
Open Black Spruce	Open Black Spruce & Open Mixed Black Spruce	5.63
Open Tall Alder	Open Tall Alder-Willow	1.28
Open Tall Shrub Birch Shrub	Open Tall Shrub Birch-Willow	9.60
Open White Spruce	Open White Spruce Forest	0.89
Closed Paper Birch	Paper Birch-Quaking Aspen Forest	8.02
Closed Quaking Aspen Forest	Paper Birch-Quaking Aspen Forest	0.54
Shrub/Bare	Shrub/Bare	0.18
Closed Quaking Aspen/White Spruce Forest	Spruce-Paper Birch-Aspen Forest	1.92
Closed Spruce/Paper Birch Forest	Spruce-Paper Birch-Aspen Forest	0.26
Closed Spruce/Paper Birch/Aspen Forest	Spruce-Paper Birch-Aspen Forest	9.33
Open Quaking Aspen/Spruce Forest	Spruce-Paper Birch-Aspen Forest	0.93
Open Spruce/Paper Birch Forest	Spruce-Paper Birch-Aspen Forest	2.75
Tussock Tundra	Tussock Tundra	9.00
Wet Sedge Meadows	Wet Sedge Meadows	5.84
Wetlands	Wetlands	6.03

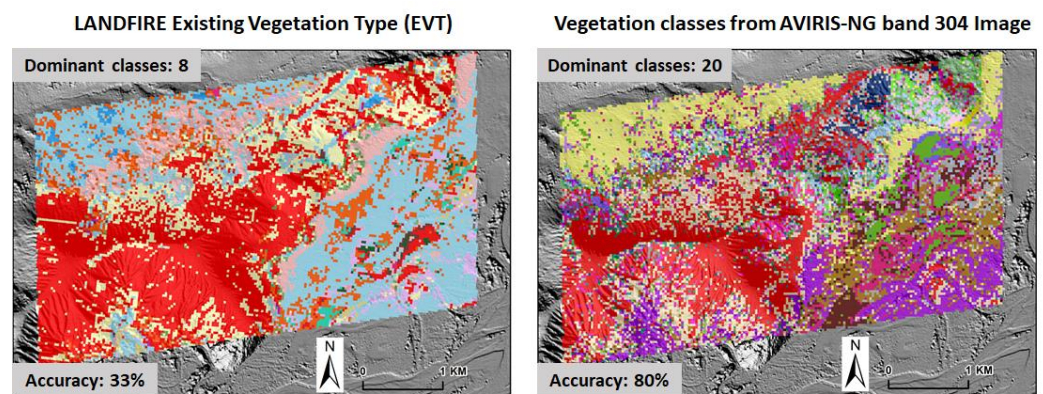


Figure 7. Comparison of vegetation map products for LF EVT (Left) and AVIRIS-NG 304 band image (Right). Colors represent distinct vegetation classes.

Table 2. Comparison of vegetation map products for LF EVT and AVIRIS-NG 304 band image pixel size, number of dominant vegetation classes, and top 3 dominant vegetation classes by percent cover.

	LANDFIRE EVT (Landsat)	AVIRIS-NG 304-Band Image + DEM Veg. Class
Pixel size	30 m	~5 m
Number of Dominant classes with % cover > 1	8	20
Top 3 dominant classes (% cover):	1. Birch-Aspen forest (33) 2. Black spruce forest (26) 3. Birch-Willow shrubland (15)	1. Closed Birch forest (16) 2. Open White Spruce forest (9) 3. Closed tall shrub (9)

Table 3. Classification accuracy for vegetation and fuel type classification from different source data at BCEF. “-” indicates data wasn’t available for calculation.

Source Data	Vegetation Classification Accuracy (%)	Fuel Type Classification Accuracy (%)	Cohan’s Kappa
LF EVT	33	-	-
Landsat + DEM	65.2	74.2	0.55
AVIRIS-NG PCA image + DEM	64.1	71.9	0.56
AVIRIS-NG 304 band image	80	81.5	0.7

3.2. CPRW

Using the random forest classifier 18 different vegetation types and 14 fire fuel types were mapped from the CPRW AVIRIS-NG data. Both of the products at CPRW had a fair agreement ($Kappa > 0.2$) based on Cohen’s Kappa. The LF EVT map had a 20% accuracy based on our field plots. The Landsat image used in LF EVT at CPRW was likely collected in the winter because vegetation was classified as snow/ice. For this site, we achieved the highest accuracy for the vegetation type (overall accuracy: 69%) and fuel types (overall accuracy: 74%) generated from the 5 PCA bands+DEM. Using the 304 bands AVIRIS-NG data, we achieved an overall accuracy of 56% for vegetation types and 61% for fuel types map products (Table 4).

Table 4. Classification accuracy for vegetation and fuel type classification from different source data at CPCWR. “-” indicates data wasn’t available for calculation.

Source Data	Vegetation Classification Accuracy (%)	Fuel Type Classification Accuracy (%)	Cohen’s Kappa
LF EVT	20	-	-
AVIRIS-NG PCA image + DEM	69	74	0.4
AVIRIS-NG 304 band image	56	61	0.36

4. Discussion

The existing vegetation type (LF EVT) of the Alaskan boreal forest were created from Landsat multispectral satellite imagery (pixel size: 30 m) that lack spatial and spectral resolution essential to capture the diversity and granularity of vegetation classes and fuel classes needed for fuel and fire management at local scales compared to AVIRIS-NG (~5 m). The LF products also lack sufficient field data to accurately classify vegetation types [24]. As a result, the available fuel maps are inadequate for effective management of active fires and firefighting resources. An example in which LF is inadequate is at CPRW where a large area of vegetation is classified as snow/ice. Using AVIRIS-NG hyperspectral data (pixel size: 5 m) we were able to produce improved (highly accurate and detailed) fuel map products for BCEF (Figure 8) and CPRW (SF3) sites. The vegetation maps of BCEF derived from AVIRIS-NG (304 bands and 5 band PCA image) had an accuracy of 80% and 74% at a fuel level compared to the 33% accuracy of LF EVT map. DeVelice also reported

similar lower accuracy of the LF EVT map (39% based on Forest Inventory and Analysis data) over the Chugach National Forest (located in southcentral Alaska), the second largest national forest in the U.S. [23]. Our fire map also identified 20 dominant classes (percent cover >1%) while the LF EVT only identified eight dominant classes within the BCEF. We demonstrated that hyperspectral data is capable of classifying boreal vegetation in greater detail (Viereck level IV) and at a higher accuracy than products created from Landsat 8. We observed that the random forest classifier yielded different accuracy using the 304 bands vs the five PCA bands coupled with the Arctic DEM. The random forest classifier using the 304 bands resulted in 81.5% accuracy at BCEF and a 60.7% accuracy at CPRW at a fire fuel level. While the PCA bands had a 72% accuracy at BCEF and a 73.8% accuracy at CPRW at a fire fuel level. This could be a result of different vegetation species and vegetation diversity at these sites. The 304 bands likely performed better at BCEF because of the larger number of vegetation classes here (25) compared to CPRW (18). It appears that the random forest classifier performs better on 304 bands when the vegetation diversity is higher. The PCA bands generated products with higher accuracy for sites with less vegetation classes and did worse identifying classes from sites with a larger number of vegetation classes. When vegetation diversity is low the 304 bands may be too much data to accurately differentiate vegetation classes compared to the five PCA bands. This shows the PCA bands are still able to accurately classify boreal vegetation while also reducing the data volume.

304 Bands Random Forest Results

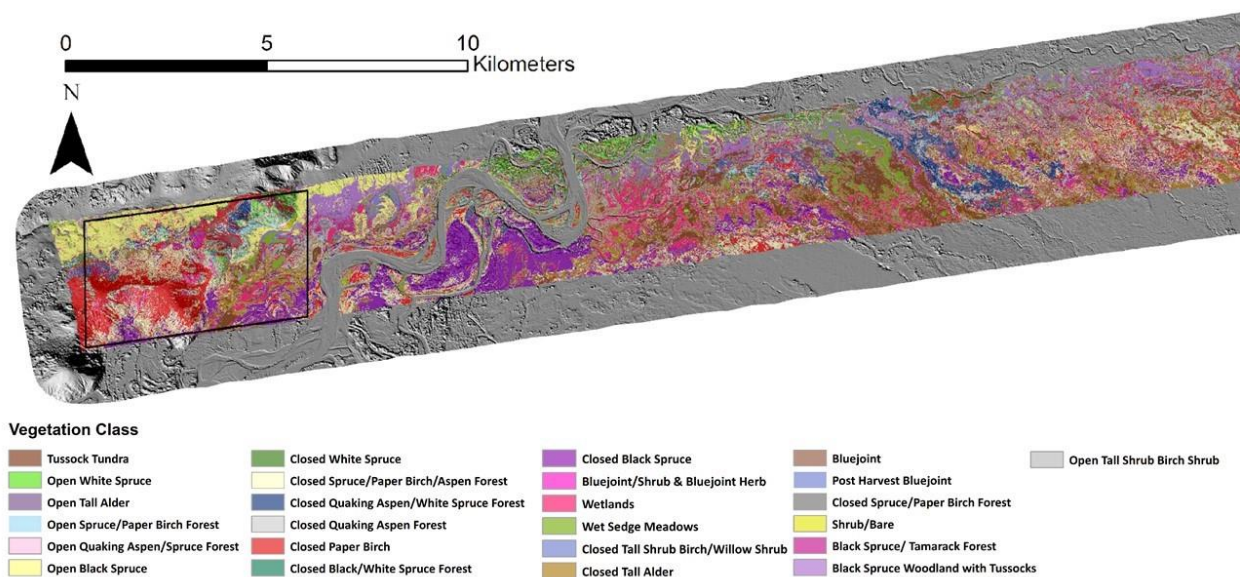


Figure 8. Vegetation Map created from 304 AVIRIS-NG bands using the Random Forest classifier. This product had a ~80% accuracy at Viereck level IV; ~82% accuracy at Alaska Fuel Model Guide Task Group (2018) fuel type.

At BCEF the LS + DEM over classified the Black Spruce Woodland with Tussocks compared to the 304-band AVIRIS-NG image (Table 3 and Table S1). The PCA + DEM over classified the Open Spruce/Paper Birch and Black Spruce Woodland with Tussocks classes compared to the 304-band AVIRIS-NG image (Table 3 and Table S2). At CPRW the 304-band AVIRIS-NG image over classified the Closed White Spruce Forest while under classifying Open Black Spruce Forest and Open Low Shrub Birch/Willow compared to the PCA + DEM (Table 5 and Table S6). This over and under misclassification may result in a lower product accuracy.

Table 5. Classified CPRW AVIRIS-NG PCA image + DEM percent area by vegetation classes.

Vegetation Type	Fuel Type	Cover (%)
Black Spruce Woodland with Tussocks	Black Spruce Woodland w/Tussocks	2.34
Black Spruce/Tamarack Forest	Black Spruce-Tamarack Forest	1.22
Closed Tall Alder	Closed Tall Alder-Willow	12.67
Closed White Spruce Forest	Closed White Spruce Forest	3.36
Dwarf Tree Black Spruce Scrub	Dwarf Tree Black Spruce Scrub	1.66
Open Black Spruce Forest	Open Black Spruce & Open Mixed Black Spruce	18.96
Open Low Shrub Birch/Willow	Open Low Shrub Birch—Ericaceous Shrub Bog and Open Low Shrub Birch—Willow	14.80
Open Paper Birch Forest	Open Paper Birch Forest	3.91
Open Quaking Aspen Forest	Open Quaking Aspen Forest	9.25
Open Tall Alder Shrub	Open Tall Alder-Willow	3.60
Open Tall Willow Shrub	Open Tall Alder-Willow	1.25
Closed Paper Birch Forest	Paper Birch-Quaking Aspen Forest	1.94
Closed Quaking Aspen Forest	Paper Birch-Quaking Aspen Forest	4.82
Closed Spruce/Paper Birch Forest	Spruce-Paper Birch-Aspen Forest	3.79
Open Quaking Aspen/Spruce Forest	Spruce-Paper Birch-Aspen Forest	7.44
Open Spruce/Paper Birch Forest	Spruce-Paper Birch-Aspen Forest	3.17
Tussock Tundra	Tussock Tundra	0.94
Wet Sedge Meadow	Wet Sedge Meadow	4.89

The common misclassification in our fire fuel maps were closed fuel types being misclassified as open fuel types of the same vegetation composition and vice versa (i.e., closed black spruce misclassified as open black spruce). The second type of misclassification observed was a pure fuel type being misclassified as a mixed fuel type and vice versa (i.e., Closed quaking aspen misclassified as closed quaking aspen/spruce). Lastly coniferous fuel type was misclassified as another coniferous fuel type (i.e., Closed white spruce misclassified as closed black spruce). The AVIRIS-NG imagery has the ability to limit these misclassifications. For example, at BCEF the Open Spruce/Paper Birch Forest class was mapped correctly 100% of the time and no other plots were misclassified as the Open Spruce/Paper Birch Forest in the 304-band AVIRIS product (Table S6). While out of the 11 random points classified as Open Spruce/Paper Birch Forest in the Landsat product, 6 of the points were incorrectly mapped in this class (Table S4). Another example is Open Spruce class at BCEF; it was mapped correctly with an accuracy of 92% ($n = 13$) in the 304-band AVIRIS product while in the Landsat 8 product the accuracy for this class was 85%. The error matrices can be found in Supplementary Materials (Tables S4–S8).

One downside of using AVIRIS-NG imagery to create vegetation and fire fuel maps is the data is collected from a fixed winged aircraft and has limited coverage. Although satellite multispectral sensor images lack spatial and spectral resolution and the derived map products usually have lower accuracy, they have global coverage allowing for fuel maps to be created almost anywhere. Another limitation of these fuel maps is that understory vegetation, moisture, and solar radiation are not considered. All of these factors greatly impact fuel's flammability. Vegetation changes in the boreal forest due to natural succession can take decades to occur but can rapidly change because of a natural disturbance such as fires, permafrost thaw, blowdowns, floods, droughts, and insect and pathogen outbreaks that alter the fuel properties [38,39]. Therefore, fire fuel maps will need to be updated using AVIRIS-NG or similar hyperspectral camera at 5–10 years interval to keep up with the boreal forest vegetation change cost-effectively and the resulting fuel product to be useful for fire managers.

This study shows that much improved and highly accurate fuel maps of boreal forest can be generated from hyperspectral data. Our products ability to map fuel/vegetation at stand scale leads to a highly detailed product that is generally lacking across the state and will be further useful for fire managers. Today's fire management involves use of sophisticated fire spread models such as FARSITE and FS Pro to reliably predict the

potential fire behavior and spread [40], but the accurate fuel information, which is essential for these predictions, is often the most limiting factor [24]. The method and findings of this study inform how to create accurate local area fuels maps. In addition to active fire management, accurate fuels maps are essential to develop strategic fire mitigation practices. For example, identifying areas of high fire risk and major paths of fire spread can be used along with values at risk to inform the fuels treatment and management around communities in the Wildland-Urban-Interface to enhance community resilience to fire risk. Research shows that fuel breaks (clearing between populated areas and wild lands) can provide an incredibly cost-effective and efficient tool for fire suppression [41,42]. For example, when fuel breaks in Alaska's Kenai Peninsula were evaluated (after three different fires), the treated areas had less intense surface fires [41]. These fuel breaks also expand the tactical options that managers use on fires near communities (e.g., 2019 Shovel Creek fire in outskirt of Fairbanks and 2019 Swan Lake fire in the outskirt of Soldotna). When fuel treatments are present on public lands, nearby homeowners are more willing to spend time and money on improving their own defensible space [41]. Using AVIRIS-NG to map moisture and running spectral unmixing (mapping percent conifers and grass in a pixel) will further improve the effectiveness of predicting fire behavior. This study serves as a benchmark for creating vegetation and fuel maps across the Alaskan boreal forest domain using scaled up and simulation techniques. The improvement of boreal forest vegetation and fuel type maps will help improve the accuracy of fire spread models and can be used to help improve research on habitat use and ecosystem services.

5. Conclusions

We produced a significantly improved and detailed vegetation and fuel type map products of BCEF and CPRW using AVIRIS-NG hyperspectral data coupled with the Arctic DEM and field data. This research demonstrated that AVIRIS-NG data can be used to accurately map Alaskan boreal forest vegetation at a finer scale than Landsat data. The products derived from AVIRIS-NG were also mapping fuel and vegetation types in more detail than the LF EVT. At BCEF our map 304 band image product has an overall accuracy of 80% at a Viereck level IV (Alaska Vegetation Classification) which is higher than the 33% accuracy of the LF EVT map. Our product at BCEF was able to identify 20 dominant classes (percent cover >1%) while the LF EVT only identified 8 dominant classes (Table 2). The more classes you have at a site using all essential bands will perform the best while the PCA performs better with less classes. Overall, both methods should be tested at a new site. The fuel maps created from this study can be used by fire managers to properly prepare for local fire events and land managers to determine species habitat and ecosystems services. This study served as a stepping stone for using scaling up and simulation techniques to create fire fuel map products for the entirety of the Alaskan boreal forest.

Supplementary Materials: The following are available online at <https://www.mdpi.com/2072-4292/13/5/897/s1>, Figure S1: Vegetation Map created from Landsat 8 using the Random Forest classifier. This product had a ~65% accuracy at Viereck level IV; ~74% accuracy at Alaska Fuel Model Guide Task Group (2018) fuel type. Figure S2: Vegetation Map created from AVIRIS PCA bands using the Random Forest classifier. This product had a ~64% accuracy at Viereck level IV; ~72% accuracy at Alaska Fuel Model Guide Task Group (2018) fuel type. Figure S3: Vegetation Map created from AVIRIS PCA bands using the Random Forest classifier. This product had a ~69% accuracy at Viereck level IV; ~74% accuracy at Alaska Fuel Model Guide Task Group (2018) fuel type. Figure S4: Vegetation Map created from 304 AVIRIS bands using the Random Forest classifier. This product had a ~56% accuracy at Viereck level IV; ~61% accuracy at Alaska Fuel Model Guide Task Group (2018) fuel type. Table S1: A list of vegetation types (fuel types) and their area percent cover mapped from LS + DEM at BCEF. Table S2: A list of vegetation types (fuel types) and their area percent cover mapped from AVIRIS-NG PCA image + DEM at BCEF. Table S3: Classified CPRW AVIRIS-NG 304 band image percent area by vegetation classes. Table S4: Vegetation type error matrix table on the random forest 5 band PCA AVIRIS BCEF product Table S5: Vegetation type error matrix table on the random forest Landsat BCEF product. Table S6: Vegetation type error matrix table on the random

forest 304 band AVIRIS BCEF product. Table S7: Vegetation type error matrix table on the random forest 304 band AVIRIS CPCWR product. Table S8: Vegetation type error matrix table on the random forest 5 band PCA AVIRIS CPCRW product.

Author Contributions: Conceptualization, C.W.S., S.K.P.; methodology, C.W.S., S.K.P.; validation, C.W.S.; formal analysis, C.W.S.; writing—original draft preparation, C.W.S., S.K.P.; writing—review and editing, C.W.S., S.K.P., F.J.M., U.S.B.; visualization, C.W.S. All authors have read and agreed to the published version of the manuscript.

Funding: This material is based upon work supported by the National Science Foundation under award #OIA-1753748 and by the State of Alaska.

Institutional Review Board Statement: Not applicable.

Informed Consent Statement: Not applicable.

Data Availability Statement: Not applicable.

Acknowledgments: Thanks to Jennifer Barnes, Teresa Hollingsworth, Jamie Hollingsworth and Robert Ziel for feedback on our research. Thanks to Anushree Badola, Colleen Haan and Robert Haan for assisting in fieldwork. Thanks to the NASA ABoVE for collecting and allowing access to AVIRIS-NG scenes. AVIRIS-NG data collected from the NASA ABoVE project can be found at <https://daac.ornl.gov/resources/tutorials/search-above-data/>. Thanks to Polar Geospatial Center for creating and allowing access to the Arctic DEM. The Arctic DEM can be found at <https://www.pgc.umn.edu/data/arcticdem/>.

Conflicts of Interest: The authors declare no conflict of interest. The funders had no role in the design of the study; in the collection, analyses, or interpretation of data; in the writing of the manuscript, or in the decision to publish the results.

Abbreviations

AVIRIS-NG	Airborne Visible/Infrared Imaging Spectrometer Next-Generation
BCEF	Bonanza Creek Experimental Forest
CPCRW	Caribou-Poker Creeks Research Watershed
DEM	Digital Elevation Model
EVT	Existing Vegetation Type
LF	LANDFIRE
NDVI	Normalized Difference Vegetation Index
PCA	Principal Component Analysis

References

1. Alaska Department of Fish and Game. Boreal Forest in Alaska—Extent, Alaska Department of Fish and Game. Available online: <http://www.adfg.alaska.gov/index.cfm?adfg=boreal.extent> (accessed on 28 December 2020).
2. Rick, T.; Walsh, J. Alaska's Changing Environment. International Arctic Research Center. Available online: [Uaf-iarc.org/our-work/alaskas-changing-environment/](http://uaf-iarc.org/our-work/alaskas-changing-environment/) (accessed on 25 February 2021).
3. Ziel, R. 2019: Alaska's Fire Environment: Not an Average Place. International Association of Wildland Fire. Available online: <http://www.iawfonline.org/article/alaskas-fire-environment-not-an-average-place/> (accessed on 26 December 2020).
4. LANDFIRE Existing Vegetation Type. Available online: <http://www.landfire.gov/evt.php> (accessed on 28 December 2019).
5. Alaska Department of Natural Resources Division of Forestry, Alaska 2019 Fire Numbers. Available online: <http://forestry.alaska.gov/Assets/pdfs/firestats/2019%20Alaska%20Fire%20Statistics.pdf> (accessed on 25 February 2021).
6. Holland, M.M.; Bitz, C.M. Polar amplification of climate change in coupled models. *Clim. Dyn.* **2003**, *21*, 221–232. [CrossRef]
7. Box, J.; Colgan, W.T.; Christensen, T.R.; Schmidt, N.M.; Lund, M.; Parmentier, F.-J.W.; Brown, R.; Bhatt, U.S.; Euskirchen, E.S.; Romanovsky, V.E.; et al. Key indicators of Arctic climate change: 1971–2017. *Environ. Res. Lett.* **2019**, *14*, 045010. [CrossRef]
8. Kasischke, E.S.; Turetsky, M.R. Recent changes in the fire regime across the North American boreal region—Spatial and temporal patterns of burning across Canada and Alaska. *Geophys. Res. Lett.* **2006**, *33*. [CrossRef]
9. Kelly, R.; Chipman, M.L.; Higuera, P.E.; Stefanova, I.; Brubaker, L.B.; Hu, F.S. Recent burning of boreal forests exceeds fire regime limits of the past 10,000 years. *Proc. Natl. Acad. Sci. USA* **2013**, *110*, 13055–13060. [CrossRef]
10. York, A.; Bhatt, U.S.; Gargulinski, E.; Grabinski, Z.; Jain, P.; Soja, A.; Thoman, R.L.; Ziel, R. *Wildland Fire in High Northern Latitudes Arctic Report Card 2020*; Thoman, R.L., Richter-Menge, J., Eds.; NOAA: Washington, DC, USA, 2020. [CrossRef]
11. Schuur, E.A.G.; McGuire, A.D.; Schadel, C.; Grosse, G.; Harden, J.W.; Hayes, D.J.; Hugelius, G.; Koven, C.D.; Kuhry, P.; Lawrence, D.M.; et al. Climate change and the permafrost carbon feedback. *Nat. Cell Biol.* **2015**, *520*, 171–179. [CrossRef] [PubMed]

12. Bieniek, P.A.; Bhatt, U.S.; York, A.; Walsh, J.E.; Lader, R.; Strader, H.; Ziel, R.; Jandt, R.R.; Thoman, R.L. Lightning Variability in Dynamically Downscaled Simulations of Alaska's Present and Future Summer Climate. *J. Appl. Meteorol. Clim.* **2020**, *59*, 1139–1152. [[CrossRef](#)]
13. Veraverbeke, S.; Rogers, B.M.; Goulden, M.L.; Jandt, R.R.; Miller, C.E.; Wiggins, E.B.; Randerson, S.V.M.L.G.E.B.W.J.T. Lightning as a major driver of recent large fire years in North American boreal forests. *Nat. Clim. Chang.* **2017**, *7*, 529–534. [[CrossRef](#)]
14. Ahmad, S.; Pandey, A.C.; Kumar, A.; Lele, N.V. Potential of hyperspectral AVIRIS-NG data for vegetation characterization, species spectral separability, and mapping. *Appl. Geomatics* **2021**, 1–12. [[CrossRef](#)]
15. Clark, M.L.; Roberts, D.A.; Clark, D.B. Hyperspectral discrimination of tropical rain forest tree species at leaf to crown scales. *Remote Sens. Environ.* **2005**, *96*, 375–398. [[CrossRef](#)]
16. Hati, J.P.; Goswami, S.; Samanta, S.; Pramanick, N.; Majumdar, S.D.; Chaube, N.R.; Misra, A.; Hazra, S. Estimation of vegetation stress in the mangrove forest using AVIRIS-NG airborne hyperspectral data. *Model. Earth Syst. Environ.* **2020**, 1–13. [[CrossRef](#)]
17. Roberts, D.; Gardner, M.; Church, R.; Ustin, S.; Scheer, G.; Green, R. Mapping Chaparral in the Santa Monica Mountains Using Multiple Endmember Spectral Mixture Models. *Remote Sens. Environ.* **1998**, *65*, 267–279. [[CrossRef](#)]
18. Salas, E.A.L.; Subburayalu, S.K.; Slater, B.; Zhao, K.; Bhattacharya, B.; Tripathy, R.; Das, A.; Nigam, R.; Dave, R.; Parekh, P. Mapping crop types in fragmented arable landscapes using AVIRIS-NG imagery and limited field data. *Int. J. Image Data Fusion* **2020**, *11*, 33–56. [[CrossRef](#)]
19. Singh, P.; Srivastava, P.K.; Malhi, R.K.M.; Chaudhary, S.K.; Verrelst, J.; Bhattacharya, B.K.; Raghubanshi, A.S. Denoising AVIRIS-NG data for generation of new chlorophyll indices. *IEEE Sens. J.* **2020**, *1*. [[CrossRef](#)]
20. Zhang, C. Combining Hyperspectral and Lidar Data for Vegetation Mapping in the Florida Everglades. *Photogramm. Eng. Remote Sens.* **2014**, *80*, 733–743. [[CrossRef](#)]
21. Miller, C.E.; Green, R.O.; Thompson, D.R.; Thorpe, A.K.; Eastwood, M.; Mccubbin, I.B.; Olson-duvall, W.; Bernas, M.; Sarture, C.M.; Nolte, S.; et al. *Arctic-Boreal Vulnerability Experiment (ABOVE) ABOVE: Hyperspectral Imagery from AVIRIS-NG, Alaskan and Canadian Arctic, 2017–2018*; ORNL DAAC: Oak Ridge, TN, USA, 2018. [[CrossRef](#)]
22. Potter, C.S. Recovery of Vegetation Cover in Burned Ecosystems of Interior Alaska Derived from a Combination of ABoVE-AVIRIS and Landsat Imagery. In Proceedings of the AGU Fall Meeting 2019, San Francisco, CA, USA, 9–13 December 2019.
23. DeVelice, R.L. *Accuracy of the LANDFIRE Alaska Existing Vegetation Map over the Chugach National Forest; LANDFIRE Assessments; 2012; Volume 10*. Available online: https://landfire.cr.usgs.gov/documents/LANDFIRE_ak_110evt_accuracy_summary_013012.pdf (accessed on 25 February 2021).
24. Krasnow, K.; Schoennagel, T.; Veblen, T.T. Forest fuel mapping and evaluation of LANDFIRE fuel maps in Boulder County, Colorado, USA. *For. Ecol. Manag.* **2009**, *257*, 1603–1612. [[CrossRef](#)]
25. Bonanza Creek LTER Overview. Available online: <http://www.lter.uaf.edu/research/study-sites-overview> (accessed on 4 December 2020).
26. Roberts, D.; Smith, M.; Adams, J. Green vegetation, nonphotosynthetic vegetation, and soils in AVIRIS data. *Remote Sens. Environ.* **1993**, *44*, 255–269. [[CrossRef](#)]
27. *Exelis Visual Information Solutions; ENVI vs 4.8*. L3Harris Geospatial: Boulder, CO, USA, 2010.
28. EnMAP-Box Developers. EnMAP-Box 3—A QGIS Plugin to Process and Visualize Hyperspectral Remote Sensing Data. 2019. Available online: <https://enmap-box.readthedocs.io> (accessed on 25 February 2021).
29. ESRI. *ArcGIS Desktop: Release 10*; Environmental Systems Research Institute: Redlands, CA, USA, 2019.
30. Agarwal, A.; El-Ghazawi, T.; El-Askary, H.; Le-Moigne, J. Efficient Hierarchical-PCA Dimension Reduction for Hyperspectral Imagery. In Proceedings of the 2007 IEEE International Symposium on Signal Processing and Information Technology, Giza, Egypt, 15–18 December 2007; pp. 353–356. [[CrossRef](#)]
31. Alaska Fuel Model Guide Task Group. *Fuel Model Guide to Alaska Vegetation*. Unpubl. Report; Alaska Wildland Fire Coordinating Group, Fire Modeling and Analysis Committee: Fairbanks, AK, USA, 2018; p. 105.
32. Viereck, L.; Dyrness, C.; Batten, A.; Wenzlick, K. *The Alaska Vegetation Classification*; USDA Forest Service: Washington, DC, USA, 1992; pp. 278–286.
33. Chapman, D.S.; Bonn, A.; Kunin, W.E.; Cornell, S.J. Random Forest characterization of upland vegetation and management burning from aerial imagery. *J. Biogeogr.* **2009**, *37*, 37–46. [[CrossRef](#)]
34. Cutler, D.R., Jr.; Beard, K.H.; Cutler, A.; Hess, K.T.; Gibson, J.; Lawler, J.J. Random Forests for Classification in ecology. *Ecology* **2007**, *88*, 2783–2792. [[CrossRef](#)]
35. Belgiu, M.; Drăguț, L. Random forest in remote sensing: A review of applications and future directions. *ISPRS J. Photogramm. Remote Sens.* **2016**, *114*, 24–31. [[CrossRef](#)]
36. Rodriguez-Galiano, V.; Ghimire, B.; Rogan, J.; Chica-Olmo, M.; Rigol-Sanchez, J. An assessment of the effectiveness of a random forest classifier for land-cover classification. *ISPRS J. Photogramm. Remote Sens.* **2012**, *67*, 93–104. [[CrossRef](#)]
37. Prasad, A.M.; Iverson, L.R.; Liaw, A. Newer Classification and Regression Tree Techniques: Bagging and Random Forests for Ecological Prediction. *Ecosyst.* **2006**, *9*, 181–199. [[CrossRef](#)]
38. Bonanza Creek LTER Disturbance Regimes. Available online: <https://www.lter.uaf.edu/boreal-forest/disturbance> (accessed on 29 December 2020).

39. Alaska Department of Fish and Game; Succession Changing Forest Habitats. Available online: https://www.adfg.alaska.gov/static-sf/statewide/aquatic_ed/AWC%20ACTIVITIES/FORESTS%20&%20WILDLIFE/BACKGROUND%20INFORMATION/Forests%20IV_Succession%20Facts.pdf (accessed on 21 January 2021).
40. Andrews, P.; Finney, M.; Fischetti, M. Predicting Wildfires. *Sci. Am.* **2007**, *297*, 46–55. [[CrossRef](#)] [[PubMed](#)]
41. Little, J.M.; Jandt, R.R.; Drury, S.A.; Molina, A.; Lane, B. Evaluating the effectiveness of fuel treatments in Alaska. Final re-port to the Joint Fire Science Program (JFSP project no. 14-5-01-27). 2018; p. 97. Available online: <https://www.frames.gov/catalog/56829> (accessed on 21 February 2021).
42. Moghaddas, J.J.; Craggs, L. A fuel treatment reduces fire severity and increases suppression efficiency in a mixed conifer forest. *Int. J. Wildland Fire* **2007**, *16*, 673–678. [[CrossRef](#)]